Majlesi J. Electr. Eng. 2026; 20(2) : 136-149

Majlesi Journal of Electrical Engineering (MJEE)

https://doi.org/10.57647/mjee.2026.2002.10

Original Research

Hexagonal Microstrip MIMO Antenna with Defected Ground Structures for ISM/IoT Application

Farzaneh Talebi, Pejman Rezaei*, Sina Kiani

Electrical and Computer Engineering Faculty, Semnan University, Semnan, Iran

***Corresponding author:** prezaei@semnan.ac.ir

Article History

Received:
6 November 2024

Revised:
18 February 2025

Accepted:
15 May 2025

Published in Issue:
30 June 2026

Abstract:

In this manuscript, an original multiple-input multiple-output (MIMO) array antenna is proposed. The proposed array consists of two mirror-image elements placed adjacently. The proposed MIMO antenna is designed on the Rogers 4003C substrate with dimensions of $54 \times 26 \times 0.508$ mm^3. The recommended MIMO antenna exhibits a fractional impedance bandwidth of 13.79% (5.4 – 6.2 GHz), and achieves an element isolation greater than 22 dB. The proposed MIMO array demonstrates a gain of 5 dB with an efficiency of 95% at 5.8 GHz. Additionally, the MIMO array has a channel capacity loss less of than 0.2 b/s/Hz, an envelope correlation coefficient of ≤ 0.02, a diversity gains of ≥ 9.96 dB, and a mean effective gain ratio between elements of 1 dB. Due to its optimal operating frequency, high efficiency, and compact size, this antenna is an appropriate candidate for ISM/IoT applications.

Keywords: Decoupling network; Defected ground structure; ISM/IoT applications; Microstrip MIMO antenna; Mutual coupling

Cite this article: Talebi F, Rezaei P, Kiani S. Hexagonal Microstrip MIMO Antenna with Defected Ground Structures for ISM/IoT Application. Majlesi J. Electr. Eng. 2026;20(2): 136-149. https://doi.org/10.57647/mjee.2026.2002.10

1. Introduction

In recent years, wireless communications have witnessed significant revolutionary advancements. The field of wireless communication systems encompasses a wide range of topics, including the development of communication chains, waveform design, interference and traffic management, channel modeling, compensating for radio hardware imperfections, symbol and bit recovery, and the enhancement of wireless security [1, 2, 3]. In the era of digital communication, the widespread use of platforms among new generations necessitates those wireless systems provide the highest data transmission rates, robust connectivity, enhanced reliability, and strong security measures [4, 5]. In recent years, MIMO antennas have obtained significant attention in non-line-of-sight wireless communications because they can utilize multiple paths for transmitting and receiving signals [6, 7]. MIMO antennas are commonly used to enhance reliability and increase data rates, thereby reducing interference from other wireless devices [8]. MIMO antennas are suitable for communication systems like LTE and Wi-Fi [9].

One challenge of MIMO antennas is the need to decrease mutual coupling between elements. When designing MIMO antennas, this parameter must be significantly reduced to ensure each antenna operates independently and efficiently [10, 11]. Some methods for controlling mutual coupling include decoupling networks, split-ring resonators (SRRs), complementary split-ring resonators (CSRRs), varactor diodes, and electromagnetic bandgap structures [12, 13].

Varactor diodes are integrated tuning components that help control frequency and radiation patterns. They utilize a dielectric material, which enhances isolation. However, incorporating varactor diodes can increase complexity, reduce overall efficiency, and require high voltage toggling between the ON and OFF states [14]. Split Ring Resonators (SRRs) enhance antenna performance by creating a resonant effect for precise frequency calibration. Complementary Split-Ring Resonators (CSRRs) are essentially the inverse of SRRs; they provide high isolation between closely spaced antennas, reduce mutual coupling, and improve the efficiency of Multiple Input Multiple Output (MIMO) systems. However, the resonant frequency of these components is sensitive to external conditions, and there can be challenges in their design and fabrication [15, 16].

Another method for reducing mutual coupling is the use of defected ground structures (DGS). DGSs have been applied in various communication devices, such as antennas [17, 18], planar waveguides [19], sensors [20, 21, 22], filters [23, 24], oscillators [25], and biosensors [26, 27, 28], to enhance performance. In recent years, antenna designers have been focused on developing wideband and wearable antennas, particularly for MIMO antenna [29, 30, 31]. Consequently, substantial research has been conducted in the areas of reconfigurable and wearable MIMO antennas [32], as well as UWB MIMO [33], positioning them as promising options for next-generation antennas [34, 35].

In this paper, an innovative MIMO microstrip array antenna is presented. The proposed antenna consists of two incomplete hexagonal patches, both of which are fed by a 50 Ω microstrip line. The antenna is placed on the Rogers 4003C board, with a thickness of 0.508 mm, a relative permittivity of 3.38, and a loss tangent of 0.0027. The primary challenge in MIMO antennas is achieving sufficient isolation between the antenna elements. This paper discusses a solution where the antenna elements are positioned on a defected ground structure (DGS) to minimize mutual coupling while maintaining a compact dimension [36]. Consequently, the proposed MIMO antenna operates within the frequency range of 5.4 – 6.2 GHz. It offers high isolation, a compact design, and low cost, making it well-suited for Internet of Things and Industrial, Scientific, and Medical (ISM/IOT) applications.

Section 2 discusses the planning steps for a single microstrip antenna, including an analysis of the S_{11} parameters at each stage, with surface current measurements taken at 5.8 GHz. Section 3 presents the designed sample and the constructed prototype of the proposed MIMO antenna, illustrated with S-parameters and radiation patterns. Finally, section 4 details the obtained results.

2. Designing steps of single microstrip element

The modified microstrip antenna is illustrated in figure 1. The Rogers 4003C substrate is utilized due to its low cost, robustness, and availability. The initial step in designing a single microstrip antenna is to determine the patch parameters using equations (1)-(5) [37]. This research utilizes the DGS to improve isolation by altering the return path of surface current at the operating frequency, based on previous studies conducted by [38, 39, 40], and [41]. The second step involves optimizing the antenna gain by loading slot on the patch, allowing the surface current to meander while maintaining the dimensions. In the third step, a slot is added to the patch, redirecting the surface current along the patch. Consequently, this increases the bandwidth and shifts the resonance frequency closer to 5.8 GHz, optimizing the antenna for ISM/IoT applications. The final goal of this article is to design a MIMO antenna. Therefore, the ground structure is modified to enhance isolation, gain, and efficiency. Figure 2 presents the design evolution of the single-element microstrip antenna, which features a defective ground structure. It includes an analysis of the S-parameter diagram and the variations in resonant frequencies. Additionally, the simulated far-field radiation pattern and gain of the single-element antenna is 3.42 dB at 5.8 GHz. Furthermore, figure 3 illustrates the surface current distributions for the single-element antenna for both the (top/bottom layer) at a frequency of 5.8 GHz.

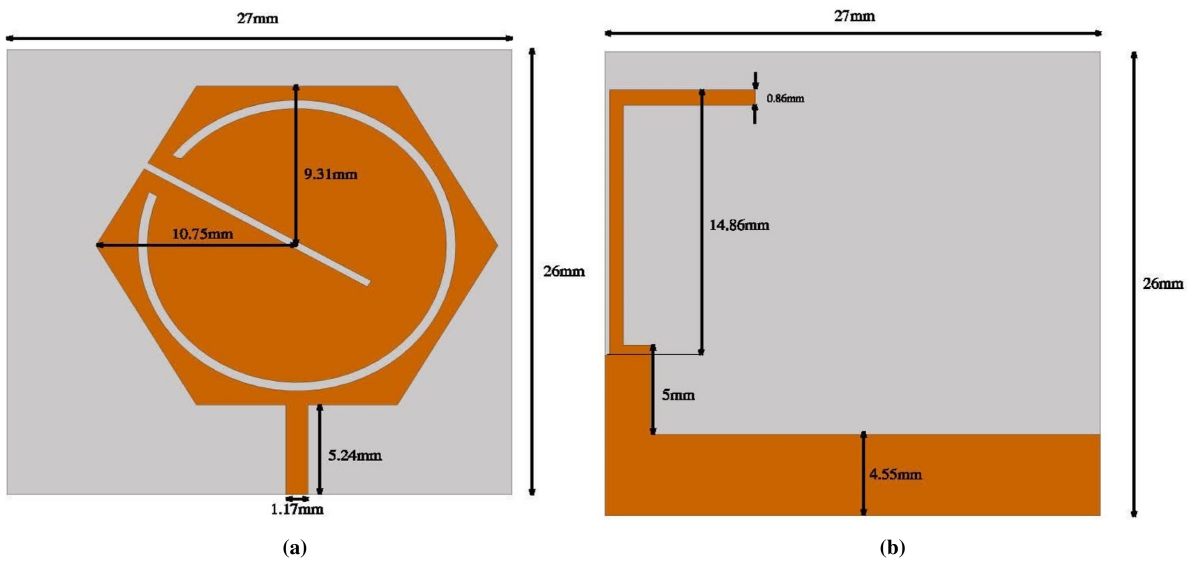

Figure 1. The Microstrip antenna, (a) top view, (b) bottom view.

https://doi.org/10.57647/mjee.2026.2002.10

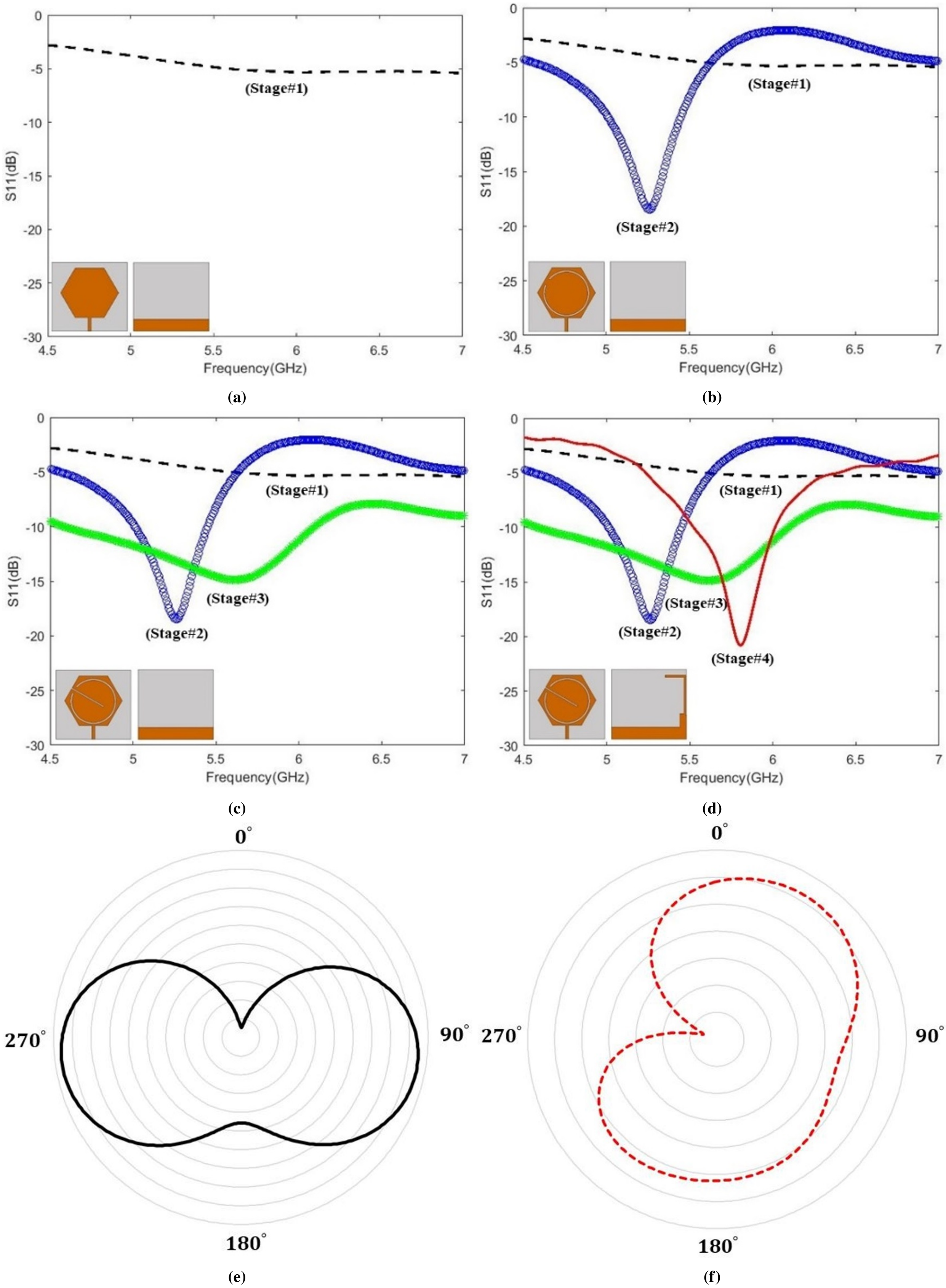

Figure 2. The single-element antenna design steps with related S_{11} diagram (a) step#1, (b) step#2, (c) step#3, (d) step#4, simulated far-field pattern at 5.8 GHz (e) H-plane (f) E-plane.

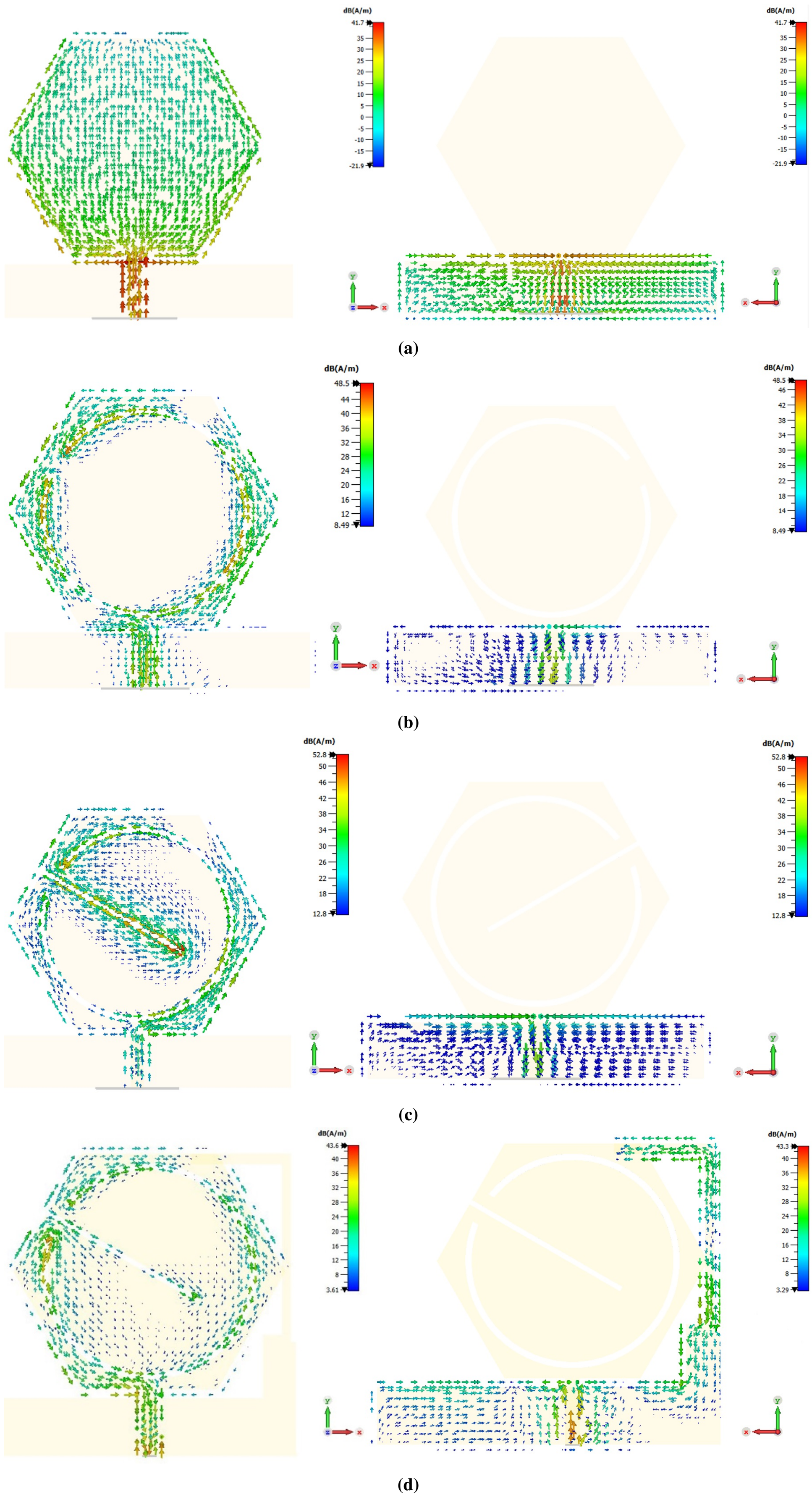

Figure 3. Distribution of surface current at 5.8 GHz (a) step#1, (b) step#2, (c) step#3, (d) step#4.

https://doi.org/10.57647/mjee.2026.2002.10

$$W = \frac{c}{2f_r}\sqrt{\frac{2}{\varepsilon_r + 1}} \quad (1)$$

where c is the velocity of light, f_r is the resonant frequency and ε_r is the dielectric constant of substrate.

$$L = L_{eff} - \Delta L \quad (2)$$

where L_{eff} is effective length of the patch given as follows:

$$L_{eff} = \frac{c}{2f_r\sqrt{\varepsilon_{eff}}} \quad (3)$$

and ΔL is the extended incremental length given as follows:

$$\Delta L = 0.412h\frac{(\varepsilon_{eff} + 0.3)(\frac{w}{h} + 0.264)}{(\varepsilon_{eff} - 0.258)(\frac{w}{h} + 0.8)} \quad (4)$$

where ε_{eff} is the effective dielectric constant given as follows:

$$\varepsilon_{eff} = \frac{\varepsilon_r + 1}{w} + \frac{\varepsilon_r - 1}{w}\left(1 + \frac{12h}{w}\right)^{-\frac{1}{2}} \quad (5)$$

Table 1 presents the calculated dimensions of the proposed patch antenna, which were derived using equations (1)-(5). These dimensions have been adjusted using CST Microwave Studio to improve the overall performance of the antenna for operation at 5.8 GHz, as illustrated in figure 1.

3. Analysis results of microstrip MIMO array

The designed and fabricated sample of the top/bottom of a proposed MIMO structure is presented in Figs. 4 and Figs. 5, respectively, which consists of double microstrip antennas arranged next to one another in a mirror pattern.

According to Figs. 6 (a,b), the bandwidth of this MIMO antenna obtained 13.79% (5.4 – 6.2 GHz), and isolation is more than 22 dB ($S_{21} \leq -22$ dB), which caused optimal performance.

The photograph of the manufactured MIMO antenna prototype in the anechoic chamber is presented in figure 7. Figures 8 (a,b) are the simulated radiation patterns on the H-plane and E-plane of the proposed microstrip MIMO radiator at 5.8 GHz. The peak gain and efficiency have obtained 5 dB and 95%, respectively. The overall simulation and measurement outcomes of the MIMO array have an appropriate overlap, however, due to the fabrication faults and different conditions, some mismatches have occurred between results. Figures 8 (c-f) demonstrate simulated radiation patterns on both the H-plane and E-plane of the proposed microstrip MIMO far-field pattern at 5.4 GHz and 6.2 GHz. Figure 8 (d) presents the antenna gain over its operational frequency range. According to the data, the antenna gains at 5.2, 5.8, and 6.2 GHz are 4.9, 5, and 4.8 dB, respectively. In the MIMO configuration, the ground planes of the antenna elements are merged and expanded to create a unified structure. Consequently, it is expected that the radiation pattern shown in Fig. 8 (b) will exhibit slight differences compared to the single-element case presented in Fig. 2 (f).

3.1 MIMO specifications

To legitimize the proposed antenna specifications as a MIMO antenna, numerous parameters for example channel capacity reduction (CCL), mean effective gain (MEG), envelope correlation coefficient (ECC), and diversity gain (DG) should be considered. All the MIMO antenna parameters have been investigated according to the S-parameters.

3.2 ECC and DG parameters

ECC can estimate the correlation and isolation between MIMO antenna elements [42]. According to the third-generation partnership project (3GPP) industrial standard, to keep an optimal implementation of a MIMO antenna, the ECC value is necessary to be below 0.5, so that each element antenna can function independently, without affecting another element [43]. The simulated and measured ECC is calculated using equation (6), with scattering parameter values [13]. Figure 9 (a) illustrates ECC, which is below 0.02 for all 5.4 – 6.2 GHz bandwidth.

$$\mathrm{ECC} = \frac{|S_{11}^{*}S_{12} + S_{21}^{*}S_{22}|}{(1 - |S_{11}|^2 - |S_{21}|^2)(1 - |S_{22}|^2 - |S_{12}|^2)} \quad (6)$$

In the MIMO antenna, diversity gain describes the obtained gain from multiple antennas in comparison to the singular element. Regularly a DG standard must be about 10 dB [44]. According to equation (7), the ECC of a MIMO array can be used to determine DG [45]. Figure 9 (a) shows that DG is close to 10 dB over the

Table 1. Dimensions of the patch antenna.

	Dielectric constant of substrate ε_r	Thickness of substrate (mm)	Effective dielectric constant ε_{eff}	Patch Width (mm)	Patch length (mm)	Extended incremental length ΔL (mm)
Original Value equations (1)-(5)	3.38	0.508	3.21	17.48	13.93	0.245
Modified Values (CST Microwave Studio)	3.38	0.508	3.24	21.5	18.62	0.248

https://doi.org/10.57647/mjee.2026.2002.10

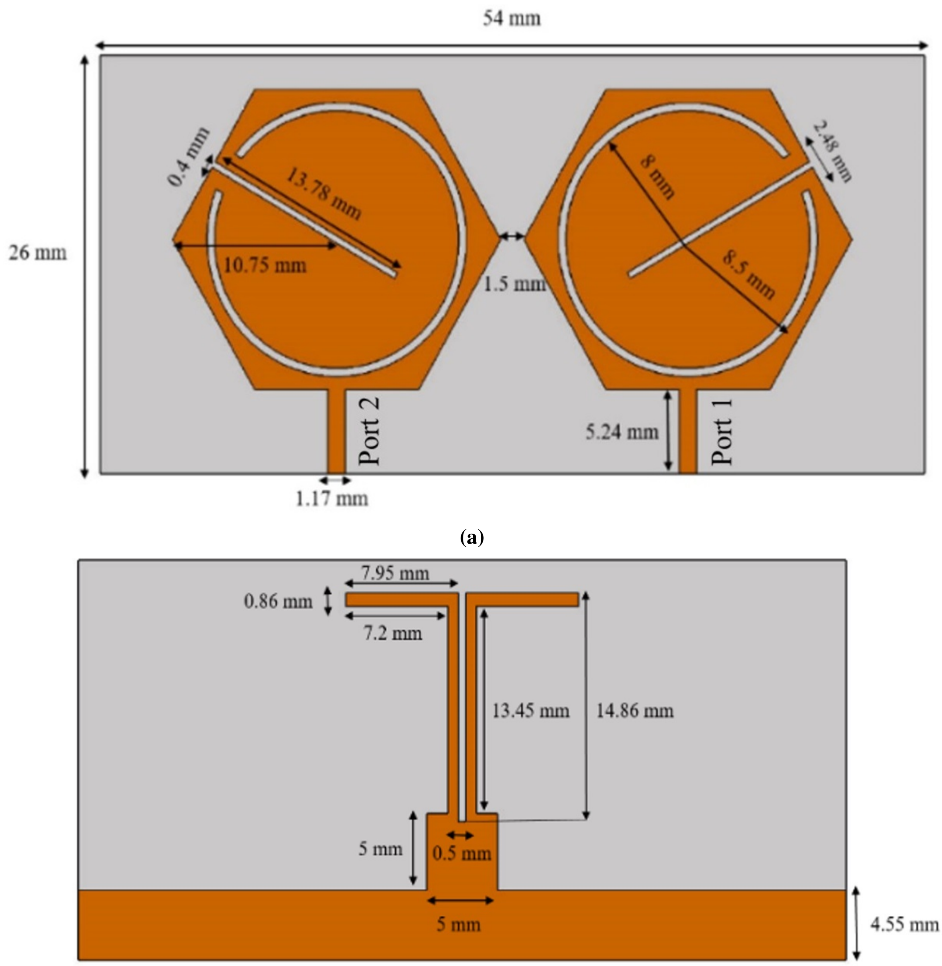

(a)

(b)

Figure 4. The proposed microstrip MIMO array with designed details: (a) top view, (b) bottom view.

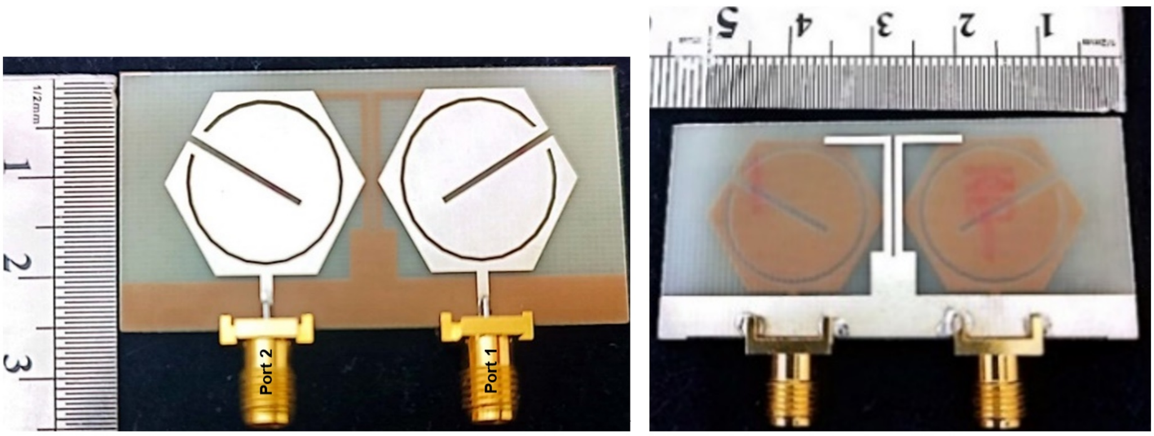

(a) **(b)**

Figure 5. The photographs of fabricated prototype microstrip MIMO array: (a) top photo, (b) bottom photo.

operating range.

$$\mathrm{DG} = 10\sqrt{1 - \mathrm{ECC}^2} \tag{7}$$

3.3 CCL parameter

Channel capacity can be expressed based on Shannon's theorem, which is an extreme possible information transfer rate through a communication channel without any interference. As a result, the system performance decline can be measured in CCL terms. The acceptable CCL values for MIMO systems are lower than 0.4 b/s/Hz. The CCL results are presented in Fig. 9 (b), which are below 0.2 b/s/Hz for the entire operational bandwidth. The CCL can be explained by equation (8), where β^R is an

https://doi.org/10.57647/mjee.2026.2002.10

antenna correlation matrix [46, 47]:

$$\mathrm{CCL(LOSS)} = -\log_2 \det \beta^R \tag{8}$$

where

$$\beta^R = \begin{bmatrix} R_{ii} & R_{ij} \\ R_{ji} & R_{jj} \end{bmatrix} \tag{9}$$

$$R_{ii} = 1 - \left(|S_{ii}|^2 + |S_{ij}|^2 \right) \tag{10}$$

$$R_{ij} = -\left(S_{ii}^* S_{ij} + S_{ji}^* S_{jj} \right) \tag{11}$$

3.4 MEG parameter

In the MIMO antenna with multipath fading situation, MEG compares the power that is given by a multiple antenna to an isotropic antenna obtained power. Matching power level, the ratio between MEGs (MEG_1/MEG_2) ought to be less than 3 dB [48]. Figure 9 (c) shows the ratio between MEGs which is 1 dB, within the standard range. MEGs can be estimated using equations (12) and (13), where $\eta_{1,rad}$ and $\eta_{2,rad}$ are the radiation coefficients in port 1 and 2, which are calculated by S-parameters for MEG_1 and MEG_2, respectively [49]:

$$MEG_1 = 0.5\eta_{1,rad} = 0.5\left[1 - |S_{11}|^2 - |S_{11}|^2\right] \tag{12}$$

$$MEG_2 = 0.5\eta_{2,rad} = 0.5\left[1 - |S_{12}|^2 - |S_{22}|^2\right] \tag{13}$$

The IoT is a vast integrated network that enables the exchange of large amounts of data at high speeds. IoT is recognized for its affordability, intermediate data rates, and an operating frequency range between 100 MHz

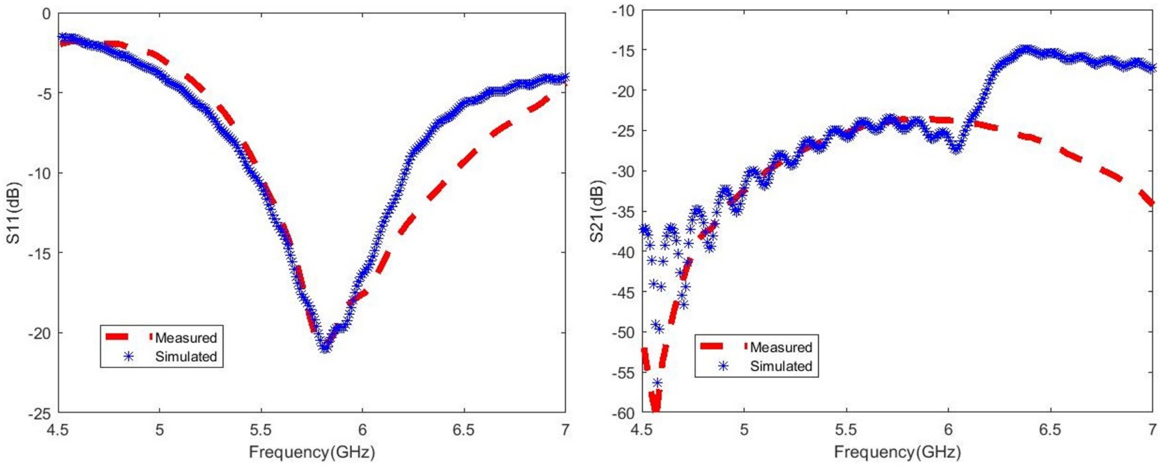

(a) **(b)**

Figure 6. Measured and simulated (a) S_{11} and (b) S_{21} parameters of MIMO antenna.

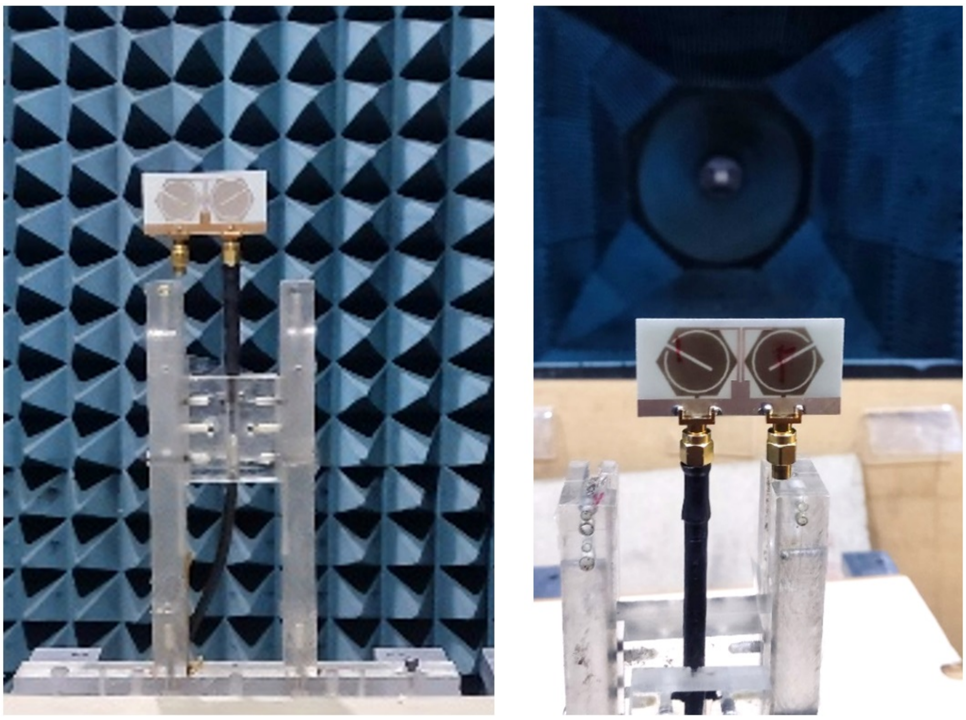

Figure 7. The photograph of the fabricated prototypes of the MIMO antenna under test in anechoic chamber.

https://doi.org/10.57647/mjee.2026.2002.10

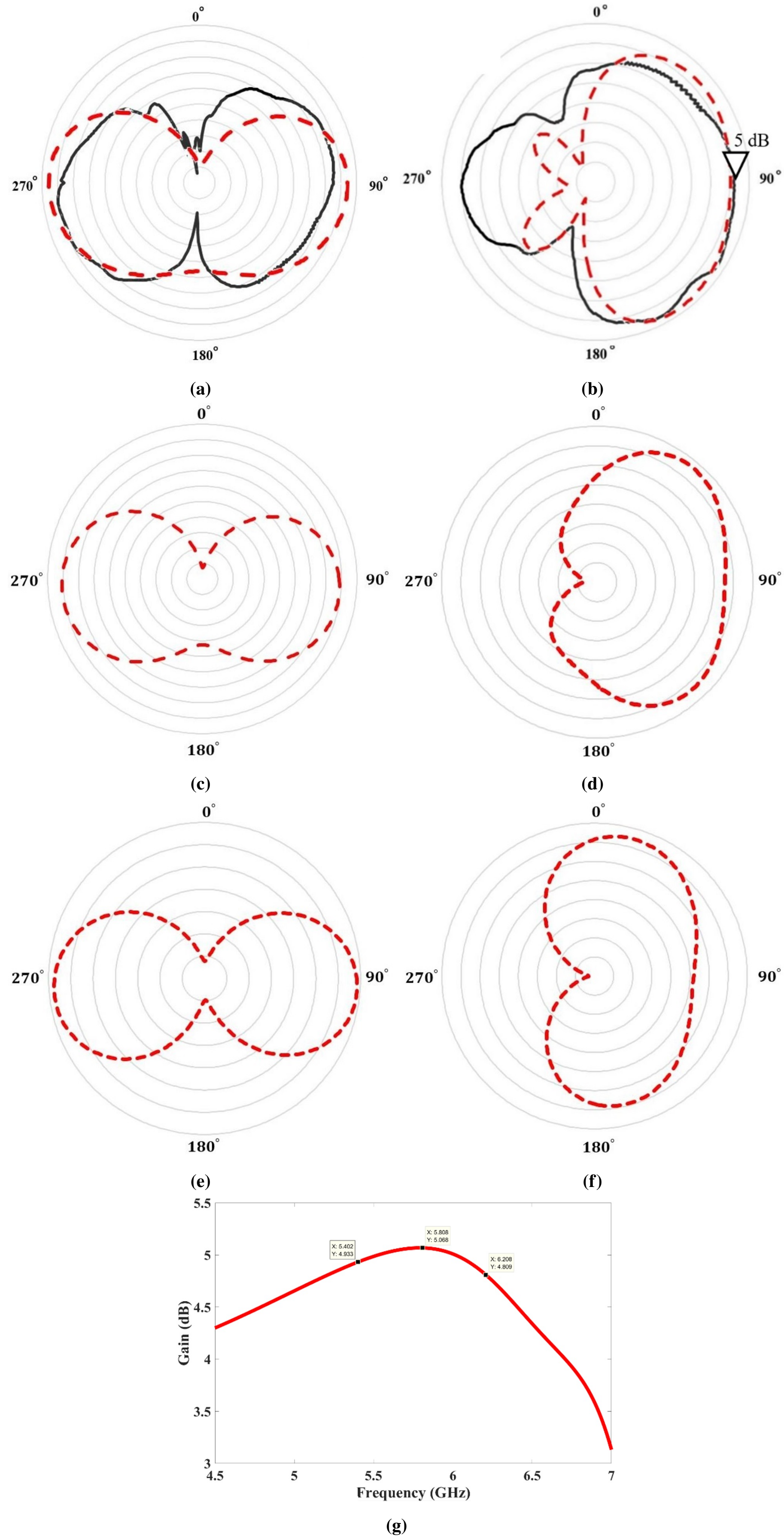

Figure 8. Measured and simulated (a) H-plane, (b) E-plane far-field pattern at 5.8 GHz, simulated of far-field pattern at 5.4 GHz (c) H-plane, (d) E-plane, and simulated of far-field pattern at 6.2 GHz (e) H-plane, (f) E-plane, (g) Diagram of antenna gain across the frequency range covered.

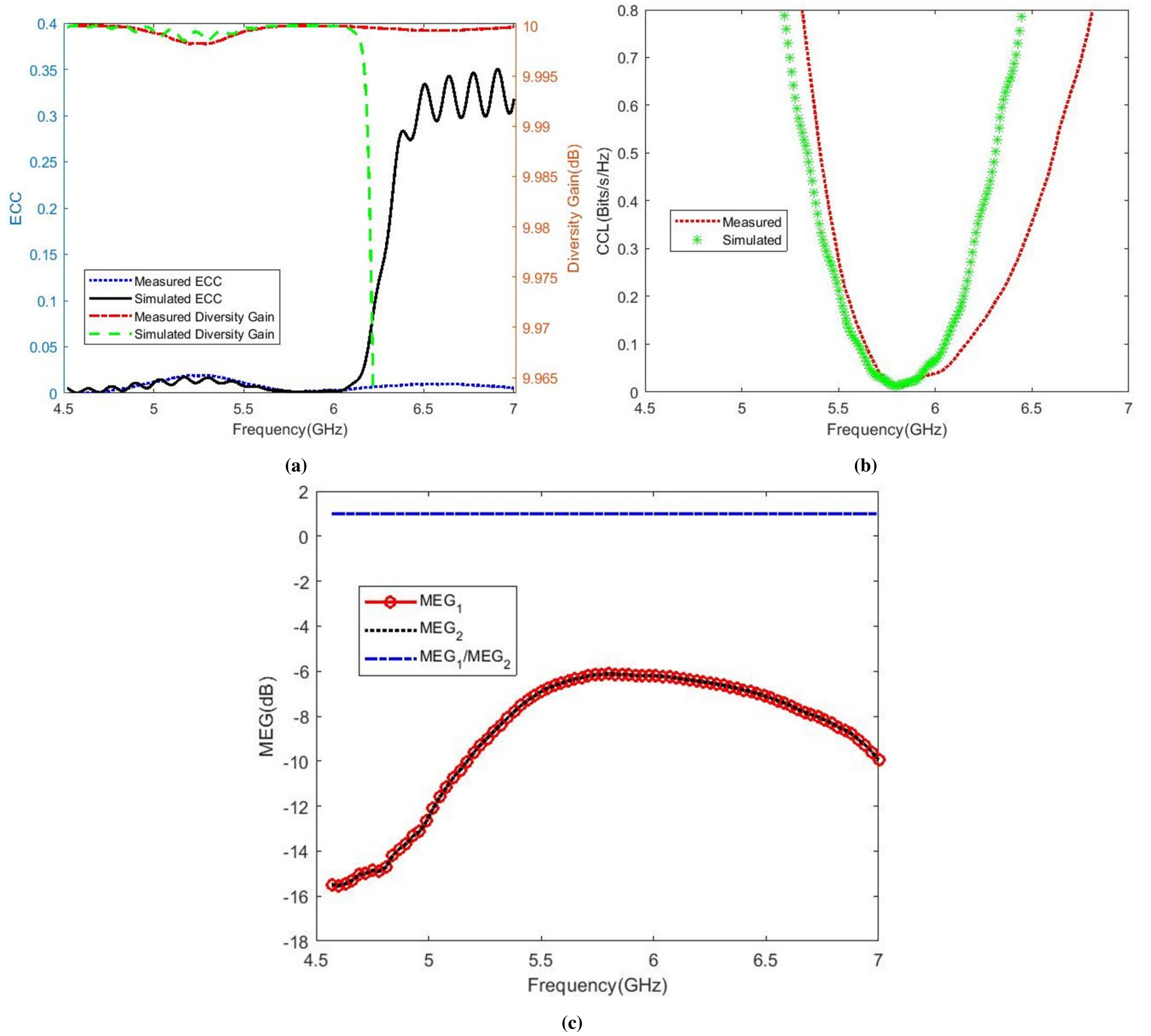

Figure 9. The proposed MIMO antenna diversity parameter (a) measured/simulated DG and ECC, (b) measured/Simulated CCL, (c) simulated MEGs.

and 5.8 GHz. IoT applications do not require specific bandwidth when operating at a frequency of 5.8 GHz [70]. The ISM band technology is primarily utilized in various applications. One of the frequency ranges available for ISM applications is 5.725 to 5.875 GHz [71, 72]. Therefore, the proposed antenna operating within a frequency range of 5.8 to 6.2 GHz with high gain and efficiency is suitable for ISM and IoT applications.

Table 2 presents a comparison of the proposed MIMO antenna with results from similar studies. The analysis reveals that the proposed antenna exhibits excellent efficiency when compared to references [51], [64], and [66]. It also demonstrates good gain relative to [42], [60], and [62]. Furthermore, in terms of isolation, it is comparable to studies [11], [63], and [65]. Consequently, the proposed MIMO antenna stands out as a suitable option for ISM/IoT applications due to its compact size, impressive gain, and high efficiency.

4. Conclusions

This study presents an original 2×1 microstrip MIMO array antenna for frequencies range between 5.4 GHz and 6.2 GHz, achieving a fractional bandwidth of 13.79%. The planned MIMO array is constructed with double mirror elements on a Rogers 4003C board, with dimensions of $54 \times 26 \times 0.508$ mm^3. The outcomes of the proposed antenna demonstrate a peak gain of 5 dB and an efficiency of 95% at 5.8 GHz frequency. Additionally, the specifications of this design have been compared with various similar works. According to these comparisons, this antenna is appropriate for ISM/IoT applications.

https://doi.org/10.57647/mjee.2026.2002.10

Table 2. Performance comparisons between different parameters of the proposed microstrip MIMO antenna with previous works.

Ref.	Frequency (GHz)	Bandwidth % (GHz)	Dimension (mm^3)	Gain (dB)	Efficiency (%)	Isolation (dB)	Application(s)
[8], 2022	2.4 3.5 5.5	8 (2.28–2.47) 11 (3.34–3.73) 38 (4.57–6.75)	$0.56 \times 0.36 \times 0.018$	1.3 2.9 4.3	–	20	ISM, 5G, WLAN
[42], 2021	2.4 6.5	87 (3–7.7)	$0.37 \times 0.25 \times 0.006$	3	78	20	Wireless
[43], 2021	3.7	24 (3.3– 4.2)	$0.45 \times 0.36 \times 0.009$	2.5	95	15	5G
[50], 2020	5.8	2 (5.72–5.89)	$1.07 \times 0.87 \times 0.029$	5.36	–	20.19	Wireless
[51], 2019	2.6	29 (2.16–2.92)	$0.34 \times 0.19 \times 0.013$	7.02	82.1	14.5	Small Satellite
[52], 2018	5.5	11 (5.25–5.92)	$1.10 \times 0.73 \times 0.157$	5	90	20	WLAN
[53], 2020	2.46	2.83 (2.43–2.5)	$0.76 \times 0.30 \times 0.012$	4.25	77.81	24.67	WLAN
[54], 2020	5.8	3.44 (5.7–5.9)	$1.06 \times 1.06 \times 0.309$	5.3	84	32	WLAN, LTE
[55], 2020	6.44	35 (5.71–8.2)	$1.70 \times 1.70 \times 0.106$	3.8	80	15	C-band
[56], 2022	2.45	25 (2.15–2.77)	$0.04 \times 0.03 \times 0.00096$	-22.7	–	30.1	Wireless capsule
[57], 2022	6	3 (5.9–6.1)	$0.80 \times 0.64 \times 0.02$	5.2	73	40	5G
[58], 2022	4	46 (3.12–5)	$0.33 \times 0.26 \times 0.021$	2.5	70	18.5	5G
[59], 2022	3.38 4.78	18.3 (2.99–3.61) 8.1 (4.53–4.92)	$0.68 \times 0.28 \times 0.016$	3.05 3.76	74.46 84.93	25 16	5G
[60], 2023	5.37	2 (5.3–5.46)	$0.68 \times 0.56 \times 0.017$	4.54	74	51.5	–
[61], 2023	5.4	10.8 (5.25–5.85)	$1.43 \times 0.89 \times 0.014$	6.5	90	25	WLAN
[62], 2023	2.5 4.5	6 (2.40–2.57) 57 (3.85–6.96)	$0.37 \times 0.25 \times 0.006$	2.65	70	15	5G, Wi-Fi
[63], 2023	3.7–7.7	112 (2.9–10.4)	$0.43 \times 0.30 \times 0.019$	5	90	20	IoT, Wearable
[64], 2022	5.8	4 (5.65–5.9)	$0.48 \times 0.99 \times 0.03$	5.6	93	17-30	WLAN
[65], 2022	2.4 5.56	12.7 (2.2–2.5) 10.7 (5.2–5.8)	$1.40 \times 0.80 \times 0.012$	–	28 16.2	20	Wi-Fi
[66], 2025	3.5 5.8	(3.01-6.5)	$0.77 \times 0.77 \times 0.018$	7.66 7.74	71.5	20	5G, WiMAX
[67], 2024	2.4	20.8 (2.2-2.7)	$0.128 \times 0.048 \times 0.002$	2.3	5.41	34	IoT
[68], 2023	3.5 6	35.7 (3.45 – 4.7) 36.6 (5.6-7.8)	$0.6 \times 0.41 \times 0.021$	1 3.8	87 85	17 26	5G, WLAN
[69], 2023	5.8	3.4 (5.7-5.9)	0.65×0.56	3.55	65	25	5G, IoT
Propoesd	5.8	13.79 (5.4–6.2)	$1.04 \times 0.50 \times 0.0098$	5	95	22	ISM, IoT

Acknowledgment

This research is funded by Semnan University, research grant 1403942. The authors would like to thank all the members of antenna laboratory at Iran Telecommunication Research Center (ITRC), for their cooperation. Also, the authors would like to thank the Editor and reviewers for their constructive comments.

Authors contributions

All authors contributed equally to the conception, design, execution, and writing of this work. All authors read and approved the final manuscript.

Availability of data and materials

The authors declare that the data supporting the findings of this study are available within the paper.

Conflict of interests

The authors assert that they do not have any identifiable conflicting financial interests or personal relationships that might be perceived to influence the work presented in this paper.

References

1. Fakharian MM, Alibakhshikenari M, See CH, and Abd-Alhameed R. "**A high gain multiband offset MIMO antenna based on a planar log-periodic array for Ku/K-band applications.**" Sci. Rep. 2022; 12:4044. DOI: 10.1038/s41598-022-07866-1
2. Khatami A, Meiguni J, AmneElahi A, et al. "**Compact via-coupling fed monopulse antenna with orthogonal tracking capability in radiation pattern.**" IEEE Antennas Wirel. Propag. Lett. 2020; 19:1443–1446. DOI: 10.1109/LAWP.2020.3005023
3. Dash JC and Sarkar D. "**Microstrip patch antenna system with enhanced inter-port isolation for full-duplex/MIMO applications.**" IEEE Access 2021; 9:156222–156228
4. Kiani S, Rezaei P, and Fakhr M. "**On-chip coronavirus shape antenna for wide band applications in terahertz band.**" J. Opt. 2023; 52:860–867. DOI: 10.1007/s12596-022-01048-y
5. Kiani S, Rezaei P, and Khajenoori M. "**Wideband sun-star shape coplanar waveguide antenna for terahertz sensing applications.**" Results Opt. 2025; 19:100815. DOI: 10.1016/j.rio.2025.100815
6. Sharma P, Tiwari RN, Singh P, et al. "**MIMO antennas: Design approaches, techniques and applications.** " Sensors 2022; 22:7813. DOI: 10.3390/s22207813
7. Niu Z, Zhang H, Chen Q, and Zhong T. "**Isolation enhancement for 1×3 closely spaced E-plane patch antenna array using defect ground structure and metal-vias.**" IEEE Access 2019; 7:119375–119383. DOI: 10.1109/ACCESS.2019.2937385
8. Bayarzaya B, Hussain N, Awan WA, et al. "**A compact MIMO antenna with improved isolation for ISM, sub-6 GHz, and WLAN application.**" Micromachines 2022; 13:1355. DOI: 10.3390/mi13081355
9. Jamal MY, Li M, and Yeung KL. "**Isolation enhancement of closely packed dual circularly polarized MIMO antenna using hybrid technique.**" IEEE Access 2020; 8:11241–11247. DOI: 10.1109/ACCESS.2020.2964902
10. Atashpanjeh E and Rezaei P. "**Innovative design for mutual coupling reduction in dual-element array antennas for ISM applications using whale optimization algorithm.** " Prog. Electromagn. Res. C 2025; 152:121–129. DOI: 10.2528/PIERC24122203
11. Omidvar A, Rezaei P, and Atashpanjeh E. "**Mutual coupling reduction with Peyton Turtle pattern nearfield surface for MIMO patch antenna.**" Frequenz 2023; 77:395–401. DOI: 10.1515/freq-2022-0150
12. Alibakhshikenari M, Babaeian F, Virdee BS, et al. "**A comprehensive survey on various decoupling mechanisms with focus on metamaterial and metasurface principles applicable to SAR and MIMO antenna systems.**" IEEE Access 2020; 8:192965–193004. DOI: 10.1109/ACCESS.2020.3032826
13. Iqbal A, Smida A, Alazemi AJ, et al. "**Wideband circularly polarized MIMO antenna for high data wearable biotelemetric devices.**" IEEE Access 2020; 8:17935–17944. DOI: 10.1109/ACCESS.2020.2967397
14. Kareem QH, Shihab RA, and Kareem HH. "**Compact dual-polarized reconfigurable MIMO antenna based on a varactor diode for 5G mobile terminal applications.**" Prog. Electromagn. Res. C 2023; 15:185–198. DOI: 10.2528/PIERC23072204
15. Sheriff N, Rahim SKA, Chattha HT, and Geok TK. "**Multiport single element MIMO antenna systems: A review.**" Sensors 2023; 23:747. DOI: 10.3390/s23020747
16. Satish K, Gunasekaran T, Ismaili SAA, and Balambigai S. "**MIMO-CSRR antenna for ISM band applications.**" Res. Square 2021 :1–10. DOI: 10.21203/rs.3.rs-342965/v1
17. Zehforoosh Y and Jalali M. "**A low mutual coupling four-port MIMO antenna for WiMAX, Bluetooth and WLAN.**" Majlesi J. Electr. Eng. 2024; 18:1–9. DOI: 10.57647/j.mjee.2024.1802.27
18. Lou RKM, Aribi T, and Sedghi T. "**Quad-band multiple input multiple output modified PIFA antenna for WLAN and LTE mobile applications.**" Majlesi J. Electr. Eng. 2023; 17:99–108. DOI: 10.30486/mjee.2023.1976700.1047

19. Kiani S and Rezaei P. "**Microwave substrate integrated waveguide resonator sensor for non-invasive monitoring of blood glucose concentration: Low cost and painless tool for diabetics.**" Measurement 2023; 219:113232. DOI: 10.1016/j.measurement.2023.113232

20. Hemmati M, Tafreshi MJ, Ehsani MH, and Alamdari S. "**Highly sensitive and wide-range flexible sensor based on hybrid BaWO4@CS nanocomposite.**" Ceramics International 2022; 48:26508–18. DOI: 10.1016/j.ceramint.2022.05.347

21. Khani S and Hayati M. "**High resolution refractive index and temperature sensor with Fano resonance in disk and parenthesis-shaped plasmonic cavities.** " Results Opt. 2025; 19:100816. DOI: 10.1016/j.rio.2025.100816

22. Ehsani MH and Alamdari S. "**Biomaterials: Fundamentals, processing, and applications. In: Ikhmayies, S.J. (eds) Advances in Biomaterials Research. Advances in Material Research and Technology.**" 2025; Springer. DOI: 10.1007/978-3-031-97481-6_1

23. Mohammadi B, Valizade A, et al. "**Design of a compact dual-band-notch ultra-wideband bandpass filter based on wave cancellation method.**" IET Microw. Antennas Propag. 2015; 9:1–9. DOI: 10.1049/iet-map.2014.0372

24. Mohammadi B, Valizade A, et al. "**New design of compact dual band-notch ultra-wideband bandpass filter based on coupled wave canceller inverted T-shaped stubs.** " IET Microw. Antennas Propag. 2015; 9:64–72. DOI: 10.1049/iet-map.2014.0484

25. Varcheh HN, Rezaei P, and Kiani S. "**A modified Jerusalem microstrip filter and its complementary for low phase noise X-band oscillator.**" Int. J. Microw. Wireless Technol. 2023; 15:1707–1716. DOI: 10.1017/S1759078723000703

26. Alipour AH, Khani S, Ashoorirad M, and Baghbani R. "**Trapped multimodal resonance in magnetic field enhancement and sensitive THz plasmon sensor for toxic materials accusation.**" IEEE Sens. J. 2023; 23:14057–14066. DOI: 10.1109/JSEN.2023.3278321

27. Jalalvand AR, Rashidi Z, and Khajenoori M. "**Sensitive and selective simultaneous biosensing of nandrolone and testosterone as two anabolic steroids by a novel biosensor assisted by second-order calibration.**" Steroids 2023; 189:109138. DOI: 10.1016/j.steroids.2022.109138

28. Khani S and Hayati M. "**Optical biosensors using plasmonic and photonic crystal band-gap structures for the detection of basal cell cancer.**" Sci. Rep. 2022; 12:5246. DOI: 10.1038/s41598-022-09213-w

29. Fakhte MHAS and Taskhiri MM. "**A broadband high gain circularly polarized magneto-electric dipole antenna with chiral metamaterial for 5G/WIMAX wireless network.**" Wireless Netw. 2024; 30:845–855. DOI: 10.1007/s11276-023-03529-9

30. Ramasamy K, Sapna BA, and Jayasheela M. "**A novel wearable monopole antenna with controlled SAR using metamaterial.** " Int. J. Microw. Wireles Technol.

31. Fakhte S and Ashouri MH. "**Broadband half mode substrate integrated waveguide H-plane horn antenna.**" Majlesi J. Electr. Eng. 2023; 17:23–28. DOI: 10.30486/mjee.2023.1970195.0

32. Lu Z, Lin H, Wang Z, Nie W, and Mu W. "**Compact ACS-fed MIMO antenna with dual-band notch characteristics for UWB applications.**" Int. J. Microw. Wireless Technol. 2024; 16:478–486. DOI: 10.1017/S1759078723001277

33. Ibrahim AA, Eltokhy A, and Daw AF. "**Four ports MIMO printed antenna with high isolation for UWB and X-band systems.**" Int. J. Microw. Wireless Technol. 2023; 15:1601–1609. DOI: 10.1017/S1759078723000296

34. Kakhki MB and Rezaei P. "**Reconfigurable microstrip slot antenna with DGS for UWB applications.**" Int. J. Microw. Wireless Technol. 2017; 9:1517–1522. DOI: 10.1017/S1759078717000034

35. Ashouri MH and Fakhte S. "**Reduction of mutual coupling between two circularly polarized magneto-electric dipole antennas using metasurface wall polarization converter for 5G application.**" Majlesi J. Electr. Eng. 2024; 18:55–63. DOI: 10.30486/mjee.2023.1991539.1180

36. Güler C and Keskin SEB. "**A novel high isolation 4-port compact MIMO antenna with DGS for 5G applications.** " Micromachines 2023; 14:1309. DOI: 10.3390/mi14071309

37. Colaco J and Lohani R. "**Design and Implementation of microstrip patch antenna for 5G applications.**" 5th Int. Conf. Commun. Electron. Syst. (ICCES) 2020 :682–685. DOI: 10.1109/ICCES48766.2020.9137921

38. Ez-Zaki E, Belahrach H, Ghammaz A, Ahmad S, et al. "**Double negative (DNG) metamaterial-based Koch fractal MIMO antenna design for sub-6-GHz V2X communication.**" IEEE Access 2023; 11:77620–77635. DOI: 10.1109/ACCESS.2023.3296599

39. Rusdiyanto D, Muslim M, Astuti DW, Adhiyoga YG, and Apriono C. "**The design of microstrip antenna using DGS and series parasitic methods for C-band applications in satellite communications.**" J. Informatics Telecommun. Eng. 2025; 8:303–312. DOI: 10.31289/jite.v8i2.12695

40. Singh P. "**Design and analysis of compact MIMO antenna for UWB applications with reduced mutual coupling.**" Authorea Preprints 2024 :1–10. DOI: 10.36227/techrxiv.173014736.66446743/v1
41. Thiruvenkadam S, Parthasarathy E, Palaniswamy SK, Kumar S, and Wang L. "**Design and performance analysis of a compact planar MIMO antenna for IoT applications.**" Sensors 2021; 21:7909. DOI: 10.3390/s21237909
42. Kulkarni J, Desai A, and Sim CYD. "**Two port CPW-fed MIMO antenna with wide bandwidth and high isolation for future wireless applications.**" Int. J. RF Microw. Comput.-Aided Eng. 2021; 31:e22700. DOI: 10.1002/mmce.22700
43. Dwivedi AK, Sharma A, Pandey AK, and Singh V. "**Two port circularly polarized MIMO antenna design and investigation for 5G communication systems.**" Wireless Pers. Commun. 2021; 120:2085–2099. DOI: 10.1007/s11277-021-08461-9
44. Saxena G, Jain P, and Awasthi YK. "**High diversity gain super-wideband single band-notch MIMO antenna for multiple wireless applications.**" IET Microw. Antennas Propag. 2020; 14:109–119. DOI: 10.1049/iet-map.2019.0450
45. Cheng Y, Liu H, Sheng BQ, and Zhu L. "**A compact 4-element MIMO antenna for terminal devices.**" Microw. Opt. Technol. Lett. 2020; 62:2930–2937. DOI: 10.1002/mop.32396
46. Kumar N and Khanna R. "**A two element MIMO antenna for sub-6 GHz and mmWave 5G systems using characteristics mode analysis.** " Microw. Opt. Technol. Lett. 2021; 63:587–595. DOI: 10.1002/mop.32626
47. Kumar S, Nandan D, Srivastava K, Kumar S, Singh H, Marey M, and Kanaujia BK. "**Wideband circularly polarized textile MIMO antenna for wearable applications.**" IEEE Access 2021; 9:108601–108613. DOI: 10.1109/ACCESS.2021.3101441
48. Das G, Sharma A, and Gangwar RK. "**Dielectric resonator based circularly polarized MIMO antenna with polarization diversity.**" Microw. Opt. Technol. Lett. 2018; 60:685–693. DOI: 10.1002/mop.31033
49. Kulkarni J, Gangwar RK, and Anguera J. "**Broadband and compact circularly polarized MIMO antenna with concentric rings and oval slots for 5G application.**" IEEE Access 2022; 10:29925–29936. DOI: 10.1109/ACCESS.2022.3157914
50. Xing H, Wang X, Gao Z, An X, Zheng HX, Wang M, and Li E. "**Efficient isolation of an MIMO antenna using defected ground structure.**" Electronics 2020; 9:1265. DOI: 10.3390/electronics9081265
51. Ameen M, Ahmad O, and Chaudhary RK. "**Wideband circularly-polarised high-gain diversity antenna loaded with metasurface reflector for small satellite applications.**" Electron. Lett. 2019; 55:829–831. DOI: 10.1049/el.2019.1645
52. Das G, Sharma A, Gangwar RK, and Sharawi MS. "**Triple-port, two-mode based two element cylindrical dielectric resonator antenna for MIMO applications.**" Microw. Opt. Technol. Lett. 2018; 60:1566–1573. DOI: 10.1002/mop.31202
53. Sharma K and Pandey GP. "**Two port compact MIMO antenna for ISM band applications.** " Prog. Electromagn. Res. C 2020; 100:173–185. DOI: 10.2528/PIERC20011504
54. Fritz-Andrade E, Perez-Miguel A, Gomez-Villanueva R, et al. "**Characteristic mode analysis applied to reduce the mutual coupling of a four-element patch MIMO antenna using a defected ground structure.**" IET Microw. Antennas Propag. 2020; 14:215–226. DOI: 10.1049/iet-map.2019.0570
55. Varshney G, Singh R, Pandey VS, and Yaduvanshi RS. "**Circularly polarized two-port MIMO dielectric resonator antenna.**" Prog. Electromagn. Res. M 2020; 91:19–28. DOI: 10.2528/PIERM20011003
56. Alazemi AJ and Iqbal A. "**A compact and wideband MIMO antenna for high-data-rate biomedical ingestible capsules.**" Sci. Rep. 2022; 12:14290. DOI: 10.1038/s41598-022-18468-2
57. Abbasi MN, Aziz A, Malik WA, Chishti AR, and Hussain R. "**A simple and modular MIMO antenna system for closely spaced patch antennas.** " Microw. Opt. Technol. Lett. 2022; 64:1210–1216. DOI: 10.1002/mop.33257
58. Kulkarni J, Gangwar RK, and Anguera J. "**Broadband and compact circularly polarized MIMO antenna with concentric rings and oval slots for 5G application.**" IEEE Access 2022; 10:29925–29936. DOI: 10.1109/ACCESS.2022.3157914
59. Sharma P, Tiwari RN, Singh P, and Kanaujia BK. "**Dual-band trident shaped MIMO antenna with novel ground plane for 5G applications.**" AEU-Int. J. Electron. Commun. 2020; 155:154364. DOI: 10.1016/j.aeue.2022.154364
60. Du Z, Zhang X, Qin P, Pu Y, and Xi X. "**Intercoupling suppression of very closely spaced MIMO antenna based on current cancellation method.**" IEEE Access 2022; 12:55103–55110. DOI: 10.1109/ACCESS.2022.3224461

61. Reddy G, Prasad NM, Dwivedi AK, et al. "**Metasurface-loaded ceramic-based MIMO antenna with high isolation and circular polarization features.**" J. Electron. Mater. 2023; 52:1305–1313. DOI: 10.1007/s11664-022-10088-w

62. Dhasarathan V, Tran TK, Kulkarni J, Garner BA, and Li Y. "**Mutual coupling reduction in dual-band MIMO antenna using parasitic dollar-shaped structure for modern wireless communication.**" IEEE Access 2023; 11:5617–5628. DOI: 10.1109/ACCESS.2023.3235761

63. Gupta P, Bharti M, and Kumar A. "**Two-element UWB antenna with multiple open slots in fountain-shaped ground for wearable and biomedical applications.** " MAPAN 2023; 38:203–215. DOI: 10.1007/s12647-022-00607-9

64. Rebbah R, Messaoudene I, Khelifi M, Hammache B, and Denidni TA. "**Enhanced isolation of MIMO cavity antenna using substrate integrated waveguide technology.**" Microw. Opt. Technol. Lett. 2022; 64:331–337. DOI: 10.1002/mop.33091

65. Wang C, Wang H, Wu P, and Hou M. "**Dual-band closed-slot MIMO antenna for terminal wireless applications.**" IEEE Trans. Antennas Propag. 2022; 70:6514–6525. DOI: 10.1109/TAP.2022.3161531

66. Ahmed H, Ameen AM, Magdy A, Nasser A, and Abo-Zahhad M. "**A Sub-6GHz two-port crescent MIMO array antenna for 5G applications.**" Electronics 2025; 14:411. DOI: 10.3390/electronics14030411

67. Gupta A, Aljaidi M, Bansal S, Mamlook REA, Kumar V, Aljohani A, Aljohani S, and Singla MK. "**Design analysis and performance enhancement of a 2-element MIMO skin-implantable antenna for IoT-based health monitoring devices.** " PLoS One 2024; 19:e0311753. DOI: 10.1371/journal.pone.0311753

68. Neamah WA, Sabbagh HMA, and Al-Rizzo H. "**A compact two-element linearly and orthogonal circularly polarized MIMO antenna system for 5G cellular and WLAN/Wi-Fi 6E application.** " IEEE Access 2023; 11:96879–96891. DOI: 10.1109/ACCESS.2023.3312122

69. Abbasi MN, Aziz A, Aljaloud KA, Chishti AR, Aladadi YT, and Hussain R. "**A close proximity 2-element MIMO antenna using optically transparent wired-metal mesh and polyethylene terephthalate material.** " IEEE Access 2023; 11:78811–78819. DOI: 10.1109/ACCESS.2023.3298568

70. Elijah AA and Mokayef M. "**Miniature microstrip antenna for IoT application.** " Mater. Today: Proc. 2020; 29:43–47. DOI: 10.1016/j.matpr.2020.05.678

71. Samy MR and Gudipalli A. "**Design circular polarized antenna at ISM band for WBAN using parasitic elements.**" Heliyon 2024; 10:e27780. DOI: 10.1016/j.heliyon.2024.e27780

72. Assogba O, Bréard A, and Duroc Y. "**A new low-cost compact antenna for the 2.45 and 5.8 GHz ISM bands.**" Appl. Sci. 2025; 15:1912. DOI: 10.3390/app15041912